Molecular Switches

DOI: 10.1002/anie.200602915

Quantum Chemical Modeling and Preparation of a Biomimetic Photochemical Switch**

Flavio Lumento, Vinicio Zanirato, Stefania Fusi, Elena Busi, Loredana Latterini, Fausto Elisei, Adalgisa Sinicropi, Tadeusz Andruniów, Nicolas Ferré, Riccardo Basosi, and Massimo Olivucci**

In memory of Fernando Bernardi

Molecular switches based on photochemical *E*/*Z* isomerization have been employed in different contexts to convert light energy into "mechanical" motion at the molecular level.[1–3] Switches based on azobenzene (Ab) have been used to control ion complexation,[4,5] electronic properties,[6] and catalysis[7] or to trigger the folding/unfolding of oligopeptide chains.[8–13] A sophisticated application of the above principle led to the preparation of chiral diarylidenes featuring a single isomerizable bond. These systems constitute examples of light-driven molecular rotors[14–17] where the chiral framework imposes a preferential direction (either clockwise or counterclockwise) of isomerization.

The design and preparation of novel building blocks differing from Ab in size, polarity, and photoisomerization mechanism constitutes an attractive research target with the aim of obtaining alternative molecular switches and, in turn, novel materials. Herein we report the results of a multidisciplinary research effort where the methods of computational photochemistry and retrosynthetic analysis/synthesis have contributed equally to prepare a switch (the indanylidene pyrroline switch (*Z*)-**1**) that mimics various aspects of

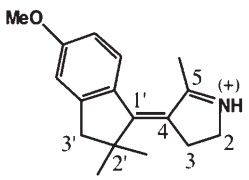

(*Z*)-**1**

the photoisomerization of rhodopsin (rhod), the visual pigment of superior animals.

The retinal protonated Schiff base chromophores of rhodopsin proteins,[18–20] a class of biological photoreceptors, constitute examples of natural *E*/*Z* switches. Such molecules undergo selective, unidirectional, and efficient photoisomerizations that, ultimately, trigger a conformational change of the protein framework. In rhod itself the π–π* excitation of the 11-*cis* form of the chromophore (PSB11) yields exclu-

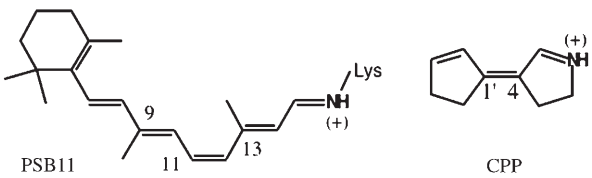

sively the all-*trans* form through a $Z \rightarrow E$ counterclockwise twist of the C11=C12 bond and occurs with a quantum yield of 0.67.[21] The attractive properties of the protein-embedded PSB11 (the isomerization selectivity, directionality, and efficiency of retinal chromophores are lost when they are irradiated in solution[19]) make it an excellent reference for

[*] Dr. F. Lumento,[+] Prof. Dr. V. Zanirato
Dipartimento di Scienze Farmaceutiche
Università di Ferrara
via Fossato di Mortara 17–19, 44100 Ferrara (Italy)
E-mail: znv@unife.it
Dr. S. Fusi, Dr. E. Busi, Dr. A. Sinicropi,[+] Prof. Dr. R. Basosi, Prof. Dr. M. Olivucci
Dipartimento di Chimica
Università degli Studi di Siena
via Aldo Moro, 53100 Siena (Italy)
Fax: (+39) 057-723-4278
E-mail: olivucci@unisi.it
Homepage: http://ccmaol1.chim.unisi.it/
Prof. Dr. M. Olivucci
Chemistry Department
Bowling Green State University
Bowling Green, OH 43403 (USA)
E-mail: molivuc@bgnet.bgsu.edu
Dr. L. Latterini, Prof. Dr. F. Elisei
Centro di Eccellenza Materiali Innovativi Nanostrutturati (CEMIN)
è Dipartimento di Chimica
Università degli Studi di Perugia
via Elce di Sotto 8, 06123 Perugia (Italy)
Dr. T. Andruniów
Institute of Physical and Theoretical Chemistry
Department of Chemistry
Wroclaw University of Technology
Wyb. Wyspianskiego 27, 50–370 Wroclaw (Poland)
Dr. N. Ferré
Laboratoire de Chimie Théorique et de Modélisation Moléculaire
UMR 6517–CNRS Universités Aix-Marseille
Case 521, Centre de Saint-Jérôme
13397 Marseille Cedex 20 (France)
[+] These authors contributed equally to this work.

[**] This work was supported by the Università di Siena (PAR02/04), FIRB (RBAU01EPMR), and COFIN2004 (Prot. 200431072_002). We are grateful to Prof. Donato Donati for help with the organic synthesis.

Supporting information for this article is available on the WWW under http://www.angewandte.org or from the author.

the design of alternative light-driven switches. In other words, while it has been established that the efficiency of the PSB11 reaction is enhanced by the complex protein environment, one may always try to design a nonnatural protonated Schiff base that, in solution, replicates the excited-state properties of the protein-embedded chromophore. This is one of the objectives of the present work.

As we will detail below, multiconfigurational quantum chemical methods, when coupled with a molecular mechanics force field, allow realistic modeling of the excited states of both protein-embedded and solution-phase protonated and N-alkylated Schiff bases (PSBs). Accordingly, these computational procedures have been used to achieve detailed descriptions of the excited states (for example, the vertical excitation energy, change in dipole moment, and magnitude of the charge transfer) and photochemical reaction paths of both synthetic and natural chromophores.

The ab initio (that is, first-principles) complete-active-space self-consistent-field (CASSCF) method[22] is a multiconfigurational method offering maximum flexibility for an unbiased description of the electronic and equilibrium structure of a molecule (that is, with no empirically derived parameters and avoiding single-reference wave functions). Furthermore, the CASSCF wave function can be used for subsequent multiconfigurational second-order perturbation theory[23] computations (CASPT2) of the dynamic correlation energy of each state, which ultimately lead to a quantitative evaluation of the excitation energies and excited-state energy differences.

Recently[24] we have implemented the ab initio CASPT2//CASSCF protocol (where equilibrium geometries and electronic energies are determined at the CASSCF and CASPT2 levels, respectively) in a quantum-mechanics/molecular-mechanics (QM/MM) scheme, thereby allowing the evaluation of the excitation energy of chromophores (treated quantum mechanically) embedded in protein and solution environments (described by the AMBER force field) with errors of a few kcal mol^{-1}. Using such a CASPT2//CASSCF/AMBER protocol, we were able to show[25] that the observed absorption and fluorescence maxima of PSB11 in rhod and in solution can be reproduced within a few kcal mol^{-1}. The same computations have also allowed the reproduction of the difference between the absorption maxima (λ^{a}_{max}) of rhod and PSB11 in methanol solution (that is, the so-called opsin shift[26]) with an error of less than 2 kcal mol^{-1}, a result indicating the consistency of the solution and protein modeling. The successful simulation of the excited-state properties of PSB11 suggests that our QM/MM method could be employed to search for synthetically accessible PSBs capable of mimicking the excited-state character of PSB11 in rhod.

In a previous report[27] we concluded that the 4-(cyclopent-2-enylidene)-3,4-dihydro-2*H*-pyrrolinium cation (CPP), featuring a single exocyclic double bond that ensures isomerization selectivity, provides the framework for the design of novel biomimetic switches. Indeed, beside the rigid dipentenylidene framework, it features a reduced PSB11-like chromophore. In order to increase the extension of the π system without increasing the number of torsional degrees of freedom of the molecule, we reasoned on the possibility of placing a third ring onto CPP. The indanylidene–pyrroline skeleton seemed the logical synthesis target. However, the impracticability of straightforward synthetic routes, like condensation between 1-indanone and pyrroline or Wittig olefination protocols, calls for an alternative synthetic route.

The salient feature of our strategy, retrosynthetically depicted in Scheme 1, is the formation of the heterocyclic ring

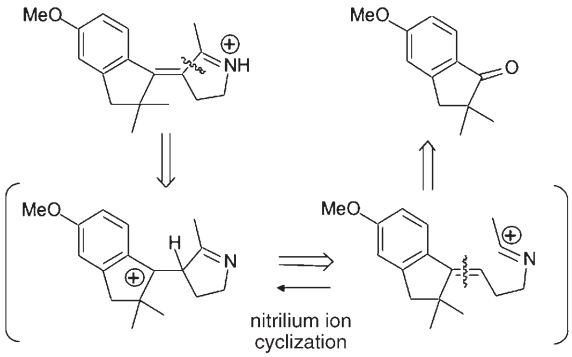

Scheme 1. Retrosynthetic analysis for production of the indanyliden-3,4-dihydro-*2H*-pyrrolinium switch **1**.

in the last step by nitrilium ion cyclization onto an indanylidene moiety, a protocol already employed to successfully prepare 3-benzylidene–pyrroline derivatives.[28] We anticipated that a methoxy group on the aromatic moiety of 1-indanone as well as the quaternarization of its C2′ carbon atom would positively influence the key cyclization step: the electron-donating group would stabilize the benzyl carbocation intermediate (see Scheme 1), the lack of hydrogen atoms at C2′ would aid the correct installation of the desired chromophoric unit onto the framework. In conclusion, retrosynthetic analysis points to the unprotonated form of (*Z*)-**1** as a realistic synthesis target.

Ab initio CASPT2//CASSCF/AMBER computations[24,25] have been used to determine the character of the excited states of a chloride–**1** ion pair in methanol solution. As a prerequisite for the interpretation of the data, we recall that in rhod[29] the (spectroscopically allowed) S_1 state of PSB11 has a dominant charge-transfer character, as originally proposed by Michl, Bonačić-Koutecký, et al.[30,31] Upon $S_0 \rightarrow S_1$ excitation, the positive charge, initially located on the N=C15 moiety, is translocated along the π skeleton (Figure 1a), thereby leading to the observed large values of $\Delta\mu$ (S_0-rhod entry in Table 1). The S_2 state is located 28 kcal mol^{-1} higher than S_1 and has a dominant covalent character and lower $\Delta\mu$ value. For PSB11 in methanol solution (S_0-PSB11 entry in Table 1), $S_0 \rightarrow S_1$ charge translocation and $\Delta\mu$ value are reduced compared to S_0-rhod. These differences are related to the decreased energy gap (16 kcal mol^{-1}) between the S_1 and S_2 states that favors state mixing.

The larger charge-transfer character of S_0-rhod with respect to S_0-PSB11 has been rationalized[25] by evaluating the effect of the protein electric field on the PSB11 cationic chromophore. In rhod the negatively charged Glu113 residue forms a salt bridge with the N=C15 Schiff base group and,

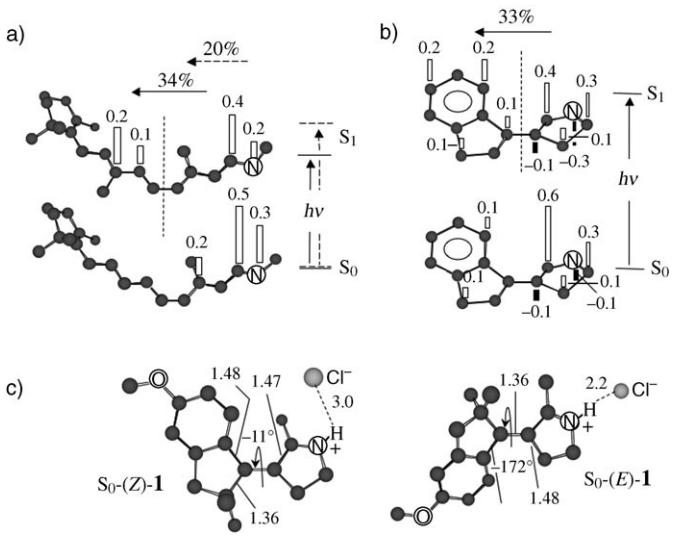

Figure 1. a) Change in the charge distribution along the retinal backbone of S_0-rhod upon vertical $S_0 \rightarrow S_1$ excitation. Partial charges are given in atomic units. The dashed arrows indicate the energy gap and charge translocation for chloride–PSB11 in methanol. b) The same data for the chloride–(*Z*)-**1** ion pair in methanol. c) CASSCF/AMBER computed equilibrium structures of the chloride–(*Z*)-**1** and chloride–(*E*)-**1** ion pairs embedded in a box (not shown) of methanol molecules. The values in degrees refer to the C5′-C1′-C4-C5 torsional angle. Bond lengths are given in Å.

Table 1: CASPT2//CASSCF/AMBER absorption (λ_{max}), change in dipole moment ($\Delta\mu$), and charge translocation (Δq) values.

Structure	Excitation	λ_{max} [nm]	$\Delta\mu$ [Debyes]	Δq[a] [au]
S_0-rhod[b]	$S_0 \rightarrow S_1$	479	11.0	−0.34
	$S_0 \rightarrow S_2$	328	3.0	−0.14
S_0-PSB11[b]	$S_0 \rightarrow S_1$	429	6.0	−0.21
	$S_0 \rightarrow S_2$	342	3.9	−0.20
S_0-(*Z*)-**1**[c]	$S_0 \rightarrow S_1$	377	8.3	−0.33
	$S_0 \rightarrow S_2$	315	1.7	−0.06
	$S_0 \rightarrow S_3$	246	1.0	0.00
S_0-(*E*)-**1**[c]	$S_0 \rightarrow S_1$	373	10.5	−0.30
	$S_0 \rightarrow S_2$	309	1.2	−0.03
	$S_0 \rightarrow S_3$	242	1.3	−0.01
S_1-(*Z*)-**1**[c]	$S_1 \rightarrow S_0$	446	6.7	−0.24
	$S_2 \rightarrow S_0$	403	5.9	−0.21
S_1-(*E*)-**1**[c]	$S_1 \rightarrow S_0$	410	10.0	−0.30
	$S_2 \rightarrow S_0$	347	0.9	−0.06
de-MeO-S_1-(*Z*)-**1**	$S_1 \rightarrow S_0$	343	7.8	−0.30
	$S_2 \rightarrow S_0$	311	1.7	−0.06

[a] Charge transfer from the pyrroline to the indanone ring for **1** and from the $=C_{12}-C_{13}=C_{14}-C_{15}=NH$ to the remaining moiety for PSB11. [b] Data from reference [25]. [c] Ion pair in MeOH with Cl^- as the anion.

thus, stabilizes the PSB11 positive charge in its S_0 location (that is, in the N=C15 region). However, the electrostatic potential generated by the remaining opsin residues (excluding Glu113) stabilizes the positive charge in the "hydrocarbon (β-ionone)" half (that is, roughly in the S_1 location) and thus significantly counterbalances the effect of the Glu113 anion. This yields a larger Δq value and a reduced $S_0 \rightarrow S_1$ excitation energy with respect to those in the solution environment as the solvent seems to quench the counterion (Cl^-) effect less efficiently.

Figure 1b gives the charge distribution computed for the ground-state equilibrium structure (S_0-(*Z*)-**1** in Figure 1c) of the chloride–**1** ion pair in methanol. The data suggest that the electronic structure of S_0-(*Z*)-**1** is more similar to that of S_0-rhod than that of S_0-PSB11. In fact (see Table 1), upon $S_0 \rightarrow S_1$ vertical excitation, S_0-(*Z*)-**1** has 33% charge transfer through its reactive C1=C4′ bond (that is, from the pyrroline to the indanone ring). This is closer in magnitude to the 34% charge transfer through the C11=C12 reactive bond seen for S_0-rhod than to the 21% seen for S_0-PSB11. A possible explanation for this similarity is provided by the following observation. Similar to S_0-rhod, S_0-(*Z*)-**1** (S_0-(*E*)-**1**) has the ability to stabilize its positive charge in a region away from the protonated N=C group by delocalizing the translocated positive charge on the substituted phenyl ring (notice the role played by the electron-releasing OMe group in such a stabilization). In conclusion, in **1** the *p*-OMe-phenyl group would "mimic" the effect of the protein residues. This conclusion is confirmed by looking at the properties of the (*Z*)-**1** analogue that is missing the *p*-OMe electron-releasing group (de-MeO-(*Z*)-**1** in Table 1). If our hypothesis is correct, the unsubstituted compound must feature, with respect to (*Z*)-**1**, reduced Δq, $\Delta\mu$, and λ_{max} values (due to an increased S_0–S_1 energy gap) as there is no *p*-OMe group to stabilize the positive charge on the phenyl ring. The values in Table 1 are in line with this prediction.

As depicted in Figure 2a, for the chloride–**1** ion pair we have been able to locate two shallow S_1 energy minima (S_1-(*Z*)-**1** and S_1-(*E*)-**1**) and a lower-lying S_1/S_0 conical intersection (CI-**1**). These structures appear to be analogues of the excited-state minimum (S_1-rhod) and conical intersection ($CI_{90°}$-rhod) reported for rhod.[25] In S_1-(*Z*)-**1** and S_1-rhod the S_1–S_2 energy gap is consistently equal to or greater than 10 kcal mol^{-1} with a weak coupling between S_1 and S_2. In S_1-PSB11 the same gap decreases to 6 kcal mol^{-1}, again, consistently with a larger state mixing for PSB11 in solution.[25]

Comparison of Figure 2a and b suggests that **1** has, for both the $Z \rightarrow E$ and $E \rightarrow Z$ reactions, a photoisomerization mechanism similar to the one documented for rhodopsin. This involves[25] 1) relaxation of the S_0-rhod to a shallow energy minimum (S_1-rhod) mainly driven by double-bond expansion and single-bond contraction but also featuring a −9° to −22° twisting of the C11=C12 reactive bond, 2) evolution along a flat S_1 energy surface towards the $CI_{90°}$-rhod conical intersection featuring an approximately 90° twisted bond, 3) $S_1 \rightarrow S_0$ decay in the conical-intersection region, and 4) barrierless relaxation along S_0 to the primary ground-state intermediate bathorhodopsin (S_0-I). Such a (nearly barrierless) path is consistent with the observed tiny fluorescence quantum yield (0.9×10^{-5})[32] and subpicosecond excited-state lifetime of the chromophore in rhod.[33]

Similar to rhod, upon excitation the S_0-(*Z*)-**1** (S_0-(*E*)-**1**) structure, which has a −11° (+8°) twisted exocyclic C1′=C4 bond (see Figure 1c) relaxes to a S_1-(*Z*)-**1** (S_1-(*E*)-**1**) structure featuring an inverted π-bond order and a −23° (+14°) twisted C1′=C4 bond. Finally, the conical intersection CI-**1** is approximately 80° twisted and it is accessed through a substantially

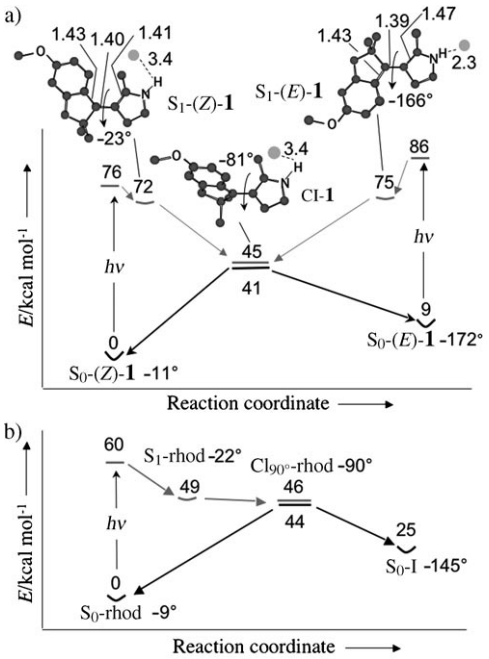

Figure 2. S_0 (black line) and S_1 (gray line) CASPT2//CASSCF/AMBER energy profiles for a) the (*Z*)-**1**→CI-**1**→(*E*)-**1**→CI-**1**→(*Z*)-**1** of Cl-(*Z*)-**1** and b) the S_0-rhod→CI→S_0-I reaction path from reference [25]. The energy values are relative to the ground state. The values in degrees refer to the C5′-C1′-C4-C5 and C10-C11-C12-C13 torsional angles for **1** and PSB11, respectively. Bond lengths are given in Å. Notice that the 9 kcal mol^{-1} difference between S_0-(*E*)-**1** and S_0-(*Z*)-**1** is approximate. See Section 2.2 in the Supporting Information).

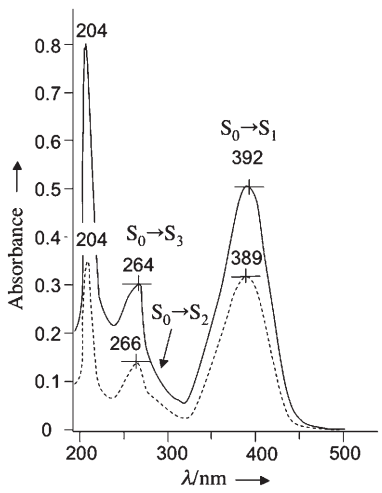

Figure 3. Room temperature absorption spectra of (*Z*)-**1** (solid line) and Me-(*Z*)-**1** (dashed line) in methanol (0.05 mM (*Z*)-**1** chloride and 0.027 mM Me-(*Z*)-**1** triflate).

barrierless path (the tiny barrier between S_1-(*Z*)-**1** and CI-**1** could not be located and it is estimated to be less than 1 kcal mol^{-1}). The barrierless path suggests that S_1-(*Z*)-**1** has a short excited-state lifetime and, thus, a very weak fluorescence. Since no other ground-state structure could be located upon relaxation from CI-**1**, we conclude that the primary photoproduct is S_0-(*E*)-**1**. This isomer has an excited-state energy surface qualitatively similar to that of S_0-(*Z*)-**1**, a fact implying that both the $Z \rightarrow E$ and $E \rightarrow Z$ photoisomerizations will occur on an ultrashort subpicosecond timescale.

The described similarities between certain electronic and geometrical features of **1** and of PSB11 in rhod suggest that the synthesis of the designed nonnatural PSB would provide access to a prototype biomimetic switch. In turn, the availability of such a compound would allow the validation of our computational procedure through comparison of the computed and observed spectral data. Thus, by starting from 5-methoxy-2,2-dimethyl-1-indanone, the free Schiff base of **1** was prepared (predominantly as the *Z* isomer) in good yield through a seven-step protocol (see the Experimental and Computational Section and the Supporting Information for details). The neutral imine was protonated with HCl to yield the switch (*Z*)-**1** or was N-methylated with methyl triflate prior to determination of its absorption spectra and photochemical behavior in methanol. N-methylated forms with a chloride counterion have also been prepared through ion-exchange protocols.

As shown in Figure 3, the absorption spectra of (*Z*)-**1** (or more precisely of a 92:8 *Z*/*E* mixture as revealed by NMR spectroscopic analysis of the starting material; see the Experimental and Computational Section) in methanol displays two bands absorbing above 250 nm. The data in Table 1 can be used to assign these bands to a given electronic transition. In fact, the computed $S_0 \rightarrow S_1$ absorption maximum (λ_{max}) falls within 20 nm of the intense band with $\lambda_{max} =$ 392 nm, which yields a computational error of less than 3 kcal mol^{-1} in excitation energy. Similarly, the observed weaker band at $\lambda_{max} = 264$ nm falls close to the computed $S_0 \rightarrow S_3$ transition. Furthermore, the $S_0 \rightarrow S_1$ and $S_0 \rightarrow S_3$ values of the oscillator strength *f* (0.55 and 0.07, respectively) are qualitatively consistent with the observed absorbance pattern. The $S_0 \rightarrow S_2$ transition is predicted to correspond to a weak band ($f = 0.06$), most probably hidden below the shoulder near 300 nm, as indicated in Figure 3.

Stationary fluorescence measurements have been carried out for the N-methylated, rather than protonated, cation to avoid the equilibrium between the protonated and unprotonated Schiff base observed for both (*Z*)-**1** and (*E*)-**1** in methanol (see the Supporting Information). Comparison of the absorption spectra for (*Z*)-**1** (chloride) and Me-(*Z*)-**1** (triflate) in Figure 3 demonstrates the invariance of the electronic structure of **1** upon alkylation. The observation of a 2.8×10^{-4} fluorescence quantum yield for Me-(*Z*)-**1** is consistent with the existence of a short-lived S_1 transient that we assign to the N-methylated form of S_1-(*Z*)-**1**. Indeed, this last species is predicted (see Table 1) to display a fluorescence λ_{max} value only 1 nm red-shifted with respect to the 445-nm λ_{max} value observed for Me-(*Z*)-**1**. Thus, the experimental fluorescence data are consistent with the data in Figure 2a in indicating a nearly barrierless $Z \rightarrow E$ photoisomerization path and, in turn, a picosecond–subpicosecond reaction timescale. This is consistent with the result of a 20-ns-resolution flash photolysis experiment on (*Z*)-**1** triflate, which showed no transient upon 335 nm irradiation.

The similarity between the reaction paths in Figure 2a and b, together with simple considerations based on a Landau–Zener model which expresses the quantum yield of a reaction in terms of nuclear velocities (as previously applied to the case of rhod)[34] for decay at CI-**1**, indicates that (*Z*)-**1** and (*E*)-**1** could potentially display high π–π* photoisomerization quantum yields. These quantities have indeed been measured for Me-(*Z*)-**1** chloride and were found to be 0.20 and 0.34 for the $Z \rightarrow E$ and $E \rightarrow Z$ processes, respectively. Such values are considerably lower than that observed for rhod. Clearly, the factors controlling the photoisomerization efficiency (including the fact that the sum of the $Z \rightarrow E$ and $E \rightarrow Z$ quantum yields is less than 1) of the investigated compound remain to be understood. This will be the subject of further studies in our laboratories.

The validity of the energy profiles of Figure 2a can be further supported on the basis of the prediction that S_0-(*Z*)-**1** and S_0-(*E*)-**1** can be photochemically interconverted with the same mechanism. Since the absorption λ_{max} value of these species is close but not identical (see Table 1), it is predicted that, upon continuous irradiation, a photostationary state will be generated whose composition depends on the irradiation wavelength. The S_0-(*E*)-**1** absorption spectrum was quantitatively determined as the difference between the spectrum of the photostationary state and the S_0-(*Z*)-**1** absorption spectrum, once the composition of the photostationary state was known.

Comparison of the (*Z*)-**1** and (*E*)-**1** spectra (see Section 3.3 in the Supporting Information) suggests, consistently with the computed λ_{max} data, a decrease of the (*Z*)-**1**/(*E*)-**1** ratio upon an increase in the wavelength. In fact, the $S_0 \rightarrow S_1$ band of (*E*)-**1** appears to be slightly blue-shifted and more intense than the corresponding (*Z*)-**1** band. Thus irradiation at a wavelength shorter than the (*E*)-**1** λ_{max} value is expected to enrich the solution in *Z* form. By contrast, irradiation at wavelengths longer than the (*Z*)-**1** λ_{max} value is expected to enrich the solution in *E* form. As shown in Table 2, the observed (*Z*)-**1**/(*E*)-**1** ratios fulfil this expectation. In particular, at 440 nm, the *E* form becomes dominant. However, due to a low $E \rightarrow Z$ thermal isomerization barrier, which could not yet been measured or computed, the generated ratio returns rapidly to the original 92:8 mixture (the composition of the thermally equilibrated solution) when the irradiation is interrupted at room temperature.

Table 2: Composition of the photostationary state (irradiation for 9 h) of **1** in methanol as a function of the irradiation wavelength.

λ [nm]	S_0-(*Z*)-**1**	S_0-(*E*)-**1**
360	1	0.28
393	1	0.34
420	1	0.74
430	1	0.90
440	1	1.44

In conclusion, we have shown that the nonnatural protonated Schiff base **1** constitutes a prototype for the development of a novel class of light-driven biomimetic switches featuring a rigid molecular framework and a fully selective *Z*/*E* photoisomerization. Most importantly, these molecules promise to expand the use of *Z*/*E* switches well beyond the applications of the Ab switch. In fact, 1) our switch is, in practice, an ion pair suitable for applications in highly polar environments while Ab is neutral with limited dipole-moment values, 2) the length of the indane–pyrroline framework is shorter than that of Ab and may be more easily integrated, for instance, in a peptide backbone, 3) the photoisomerization of **1** is controlled, exclusively, by the π–π* excited state while Ab reacts through both the n–π* and π–π* states, 4) the isomerization quantum yields measured in methanol (0.20 and 0.34 for (*Z*)-**1** and (*E*)-**1**, respectively) are not far from the n–π* quantum yields (0.35 and 0.41) observed for (*Z*)-Ab and (*E*)-Ab in water/ethanol, and in the same solvent their π–π* quantum yields are lower, 5) the isomerization mechanism of **1** only involves twisting about the exocyclic double bond while Ab has both twisting and inversion mechanisms that could dominate in different contexts, and finally 6) the ab initio CASPT2//CASSCF/AMBER modeling used in the present work is not applicable to Ab (in the absence of molecular symmetry) due to the excessive extension of its π system. We believe that these distinctive properties make **1** an attractive alternative to Ab.

Experimental and Computational Section

An exhaustive α methylation of **2a** following a reported protocol[35] opened the synthetic sequence (step a in Scheme 2). In step b, the Grignard addition reaction afforded, in 90% yield, the corresponding 1-cyclopropylindan-1-ol **3** which, by the action of 33% HBr in acetic acid (step c), smoothly underwent the expected rearrangement (79%).[36] The bromopropylidene derivative **4** was a suitable substrate to go on with the synthesis; in fact, as a 3:1 mixture of geometric isomers, it was submitted to the three steps of sequence d to yield the indanylidene compound **5** with a tethered acetamido group (63% overall yield). In step e, trimethylsilylpolyphosphate (PPSE) promoted dehydration of the secondary amide function to generate the

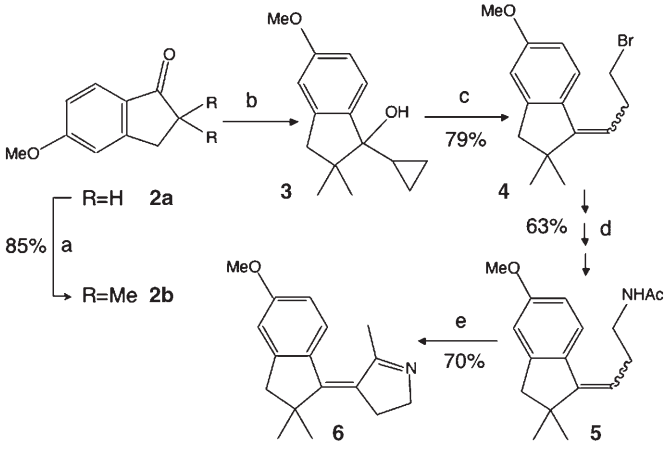

Scheme 2. Synthesis of the free Schiff base (*Z*)-**1**: a) MeI, *t*BuOK, *t*BuOH, Et_2O, reflux, 7 h; b) Mg, cyclopropylbromide, THF, reflux, 3 h; c) HBr, AcOH, 10 min; d) 1. NaN_3, DMF, 70°C, 2 h; 2. $LiAlH_4$, Et_2O, reflux, 2 h; 3. CH_3COCl, Et_3N, CH_2Cl_2; e) P_2O_5, HMDS, CCl_4, reflux, 2 h. DMF = *N*,*N*-dimethylformamide, HMDS = 1,1,1,3,3,3-hexamethyldisilazane.

pivotal nitrilium ion that, by quenching onto the exocyclic olefin moiety, eventually yielded the target compound **6**. Inspection of the NMR spectrum showed a predominant (98:8) diastereomer whose geometry appears to be *Z* on the basis of NOE experiments. Experimental reaction conditions leading to the key synthetic intermediate 1-(3-bromopropylidene)-5-methoxy-2,2-dimethylindane **4** and to the final compound 4-(5-methoxy-2,2-dimethylindan-1-ylidene)-5-methyl-3,4-dihydro-2*H*-pyrrole Schiff base **6**, as well as the spectroscopic characterization f these compounds, are reported in the Supporting Information.

Spectroscopy and photochemistry: Photoisomerization was carried out with a 900 W irradiator, *f*/3.4 monochromator (Applied Photophysics) apparatus and was followed by ^{1}H NMR spectroscopy (Bruker AC 200 spectrometer at 200.13 MHz). The composition of the photostationary state at different irradiation wavelengths was evaluated from the area ratio of the signal of the aromatic proton in the *ortho* position with respect to the exocyclic double bond (see above and the Supporting Information. UV/Vis measurements were performed by using a Hewlett Packard 8423 spectrophotometer. See the Supporting Information for further details.

Computations: The model of the *Z* and *E* switches in solution was constructed by placing the chromophore in a rectangular box of methanol molecules positioned within 10 Å from any given atom of the chromophore by using the xleap module of the Amber package.[37] To neutralize the system we added a chloride anion. The average ground-state configuration of the methanol molecules (that is, the solvent) was determined according to the following procedure. The solvent (including the counterion) was minimized for 2000 steps by using the steepest-descent method while keeping the chromophore (that is, the solute) fixed in its gas-phase configuration. In this step the partial charges of the chromophore atoms were determined with Gaussian03,[38] by using a Restrained ElectroStatic Potential (RESP) procedure at the HF/6-31G* level of theory. In the next step we performed CASSCF/6-31G*/AMBER geometry optimization to relax the coordinates of the QM chromophore, MM counterion, and solvent molecules with any atom within less than 4.5 Å from any solute atom. The positions of the remaining solvent molecules, more distant from the chromophore, were kept frozen. The QM calculations were based on a CASSCF/6-31G* level including an active space of 12 electrons in 11 π orbitals (that is, the full π system of the solute). The chosen 6-31G* basis set represented a cost/accuracy compromise yielding an excitation energy error of less than 3 kcal mol^{-1} for rhod and solution-phase PSB11.[25] CASSCF/6-31G*/AMBER geometry optimization was carried out with Gaussian03[38] and TINKER 3.9.[39] To account for a dynamical correlation energy, four root-state average CASPT2 calculations were carried out by using the MOLCAS 5.4[40] software.

Received: July 20, 2006
Published online: December 5, 2006

Keywords: ab initio calculations · molecular switches · nitrilium ion cyclization · photoisomerization · retinal chromophore

[1] Special issue: *Struct. Bonding (Berlin)* **2001**, *99* (Ed.: V. Amendola).
[2] K. E. Drexler, *Nanosystems: Molecular Machinery, Manufacturing and Computation*, Wiley, New York, **1992**.
[3] V. Balzani, A. Credi, M. Venturi, *Molecular Devices and Machines. A Journey into the Nanoworld*, Wiley-VCH, Weinheim, **2003**.
[4] S. Shinkai, Y. Kusano, O. Manabe, T. Nakaji, Y. Nishida, T. Ogawa, *J. Am. Chem. Soc.* **1980**, *102*, 5860.
[5] S. Shinkai, T. Minami, Y. Kusano, O. Manabe, *J. Am. Chem. Soc.* **1983**, *105*, 1851.
[6] B. Jousselme, P. Blanchard, N. Gallego-Planas, J. Delaunay, M. Allain, P. Richomme, E. Levillain, J. Roncali, *J. Am. Chem. Soc.* **2003**, *125*, 2888.
[7] R. Cacciapaglia, S. D. Stefano, L. Mandolini, *J. Am. Chem. Soc.* **2003**, *125*, 2224.
[8] R. Behrendt, C. Renner, M. Schenk, F. Wang, J. Wachtveitl, D. Oesterhelt, L. Moroder, *Angew. Chem.* **1999**, *111*, 2941; *Angew. Chem. Int. Ed.* **1999**, *38*, 2771.
[9] J. Bredenbeck, J. Helbing, A. Sieg, T. Schrader, W. Zinth, C. Renner, R. Behrendt, L. Moroder, J. Wachtveitl, P. Hamm, *Proc. Natl. Acad. Sci. USA* **2003**, *100*, 6452.
[10] L. Ulysse, J. Cubillos, J. Chmielewski, *J. Am. Chem. Soc.* **1995**, *117*, 8466.
[11] S. Rudolph-Böhner, M. Krüger, D. Oesterhelt, L. Moroder, T. Nägele, J. Wachtveitl, *J. Photochem. Photobiol. A* **1997**, *105*, 235.
[12] C. Renner, R. Behrendt, S. Spörlein, J. Wachtveitl, L. Moroder, *Biopolymers* **2000**, *54*, 489.
[13] S. Spörlein, H. Carstens, H. Satzger, C. Renner, R. Behrendt, L. Moroder, P. Tavan, W. Zinth, J. Wachtveitl, *Proc. Natl. Acad. Sci. USA* **2002**, *99*, 7998.
[14] N. Koumura, E. M. Geertsema, M. B. van Gelder, A. Meetsma, B. L. Feringa, *J. Am. Chem. Soc.* **2002**, *124*, 5037.
[15] N. Koumura, R. W. J. Zijistra, R. A. van Delden, N. Harada, B. L. Feringa, *Nature* **1999**, *401*, 152.
[16] N. Koumura, E. M. Geertsema, A. Meetsma, B. L. Feringa, *J. Am. Chem. Soc.* **2000**, *122*, 12005.
[17] B. L. Feringa, *Acc. Chem. Res.* **2001**, *34*, 504.
[18] R. A. Mathies, J. Lugtenburg in *Handbook of Biological Physics, Vol. 3* (Eds.: D. G. Stavenga, W. J. de Grip, E. N. Pugh), Elsevier Science B.V., Amsterdam, **2000**, p. 56.
[19] H. Kandori, Y. Shichida, T. Yoshizawa, *Biochemistry (Moscow)* **2001**, *66*, 1483.
[20] D. C. Teller, T. Okada, C. A. Behnke, K. Palczewski, R. E. Stenkamp, *Biochemistry* **2001**, *40*, 7761.
[21] H. Dartnall, *Vision Res.* **1967**, *8*, 339.
[22] B. O. Roos in *Advances in Chemical Physics; Ab initio Methods in Quantum Chemistry II* (Ed.: K. P. Lawley), Wiley, Chichester, **1987**, p. 399.
[23] K. Andersson, P.-A. Malmqvist, B. O. Roos, A. J. Sadlej, K. J. Wolinski, *Phys. Chem.* **1990**, *94*, 5483.
[24] N. Ferre, M. Olivucci, *J. Am. Chem. Soc.* **2003**, *125*, 6868.
[25] T. Andruniów, N. Ferré, M. Olivucci, *Proc. Natl. Acad. Sci. USA* **2004**, *101*, 17908.
[26] B. Honig, U. Dinur, K. Nakanishi, V. Balogh-Nair, M. A. Gavinowicz, M. Arnaboldi, M. G. Motto, *J. Am. Chem. Soc.* **1979**, *101*, 7084.
[27] D. Sampedro Ruiz, A. Migani, A. Pepi, E. Busi, R. Basosi, L. Latterini, F. Elisei, S. Fusi, F. Ponticelli, V. Zanirato, M. Olivucci, *J. Am. Chem. Soc.* **2004**, *126*, 9349.
[28] R. Gawley, S. Chemburkar, *Heterocycles* **1989**, *29*, 1283.
[29] R. Gonzales-Luque, M. Garavelli, F. Bernardi, M. Merchan, M. A. Robb, M. Olivucci, *Proc. Natl. Acad. Sci. USA* **2000**, *97*, 9379.
[30] V. Bonačić-Koutecký, J. Koutecký, J. Michl, *Angew. Chem.* **1987**, *99*, 216; *Angew. Chem. Int. Ed. Engl.* **1987**, *26*, 170.
[31] V. Bonačić-Koutecký, J. Köhler, J. Michl, *Chem. Phys. Lett.* **1984**, *104*, 440.
[32] G. G. Kochendoerfer, R. A. Mathies, *J. Phys. Chem.* **1996**, *100*, 14526.
[33] R. W. Schoenlein, L. A. Peteanu, R. A. Mathies, C. V. Shank, *Science* **1991**, *254*, 412.
[34] Q. Wang, R. W. Schoenlein, L. A. Peteanu, R. A. Mathies, C. V. Shank, *Science* **1994**, *266*, 422.
[35] T. Nishio, N. Okuda, C. Kashima, *Liebigs Ann.* **1996**, 117.

[36] R. Perrone, F. Berardi, N. A. Colabufo, M. Leopoldo, V. Tortorella, F. Fiorentini, V. Olgiati, A. Ghiglieri, S. Govoni, *J. Med. Chem.* **1995**, *38*, 942.
[37] D. A. Case, D. A. Pearlman, J. W. Caldwell, T. E. Cheatham III, J. Wang, W. S. Ross, C. L. Simmerling, T. A. Darden, K. M. Merz, R. V. Stanton, A. L. Cheng, J. J. Vincent, M. Crowley, V. Tsui, H. Gohlke, R. J. Radmer, Y. Duan, J. Pitera, I. Massova, G. L. Seibel, U. C. Singh, P. K. Weiner, P. A. Kollman, University of California, San Francisco, **2002**.
[38] Gaussian 03 (Revision B.04), M. J. Frisch, G. W. Trucks, H. B. Schlegel, G. E. Scuseria, M. A. Robb, J. R. Cheeseman, J. J. A. Montgomery, T. Vreven, K. N. Kudin, J. C. Burant, J. M. Millam, S. S. Iyengar, J. Tomasi, V. Barone, B. Mennucci, M. Cossi, G. Scalmani, N. Rega, G. A. Petersson, H. Nakatsuji, M. Hada, M. Ehara, K. Toyota, R. Fukuda, J. Hasegawa, M. Ishida, T. Nakajima, Y. Honda, O. Kitao, H. Nakai, M. Klene, X. Li, J. E. Knox, H. P. Hratchian, J. B. Cross, C. Adamo, J. Jaramillo, R. Gomperts, R. E. Stratmann, O. Yazyev, A. J. Austin, R. Cammi, C. Pomelli, J. W. Ochterski, P. Y. Ayala, K. Morokuma, G. A. Voth, P. Salvador, J. J. Dannenberg, V. G. Zakrzewski, S. Dapprich, A. D. Daniels, M. C. Strain, O. Farkas, D. K. Malick, A. D. Rabuck, K. Raghavachari, J. B. Foresman, J. V. Ortiz, Q. Cui, A. G. Baboul, S. Clifford, J. Cioslowski, B. B. Stefanov, G. Liu, A. Liashenko, P. Piskorz, I. Komaromi, R. L. Martin, D. J. Fox, T. Keith, M. A. Al-Laham, C. Y. Peng, A. Nanayakkara, M. Challacombe, P. M. W. Gill, B. Johnson, W. Chen, M. W. Wong, C. Gonzalez, J. A. Pople, Gaussian, Inc., Pittsburgh, PA, **2003**.
[39] J. W. Ponder, F. M. Richards, *J. Comput. Chem.* **1987**, *8*, 1016.
[40] K. Andersson, M. Barysz, A. Bernhardsson, M. R. A. Blomberg, D. L. Cooper, M. P. Fülscher, C. Graaf, B. A. Hess, G. Karlström, R. Lindh, P.-A. Malmqvist, T. Nakajima, P. Neogrády, J. Olsen, B. O. Roos, B. Schimmelpfennin, M. Schütz, L. Seijo, L. Serrano-Andrés, P. E. M. Siegbahn, J. Stålring, T. Thorsteinsson, V. Veryazov, P.-O. Widmark, Lund University, Sweden, **2002**.

